Numerical Modeling

Semester Report

Antonio Peters

May 26, 2016

Contents

List of Figures

Chapter 1

Introduction and Preliminaries

This report will detail the work done for the Numerical Modeling mathematics honors course. Whenever possible, decimal values will be calculated to double precision. Data will generally be stored in a *.dat* which will then be read in and plotted. The report will build up from analyzing the finite difference method, error approximation and convergence, and boundary conditions to understanding time evolutions and the Riemann problem and then will look at Gordinov's method in order to simulate high resolution shock capturing in order to solve Burgers' equation.

Chapter 2

Finite Difference

There are several different variants of the finite difference methods (FDMs), this is dependent on the stencil, the number of points being used to determine a single value. The use of a larger stencil yields a lower error, as can be seen in Figure 2.1 but also requires more computation time to generate a result.

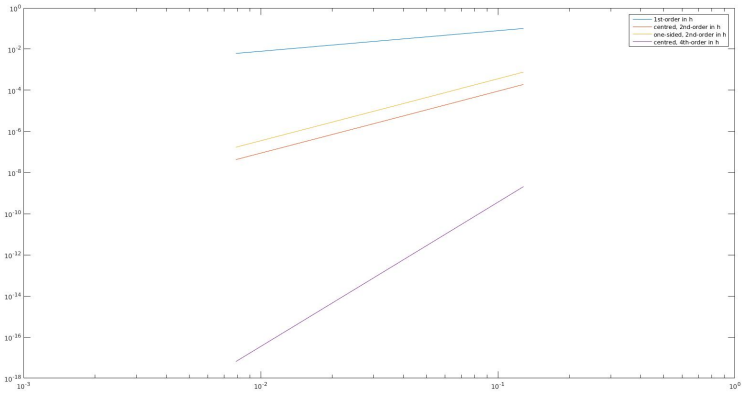

Figure 2.1: Comparison of Errors in FDM variants in log plot

2.1 First Derivatives

The FDM uses Taylor expansion to approximate the derivative of a function of finite points using the surrounding points such that $dv_i \approx \frac{df(x_i)}{dx}$.

The most basic of these is the first order FDM, given by Equation 2.1. It first order as the error in the function is relative to the spacing in the first

order, $\epsilon \approx h$.

$$dv_i = \frac{v_{i+1} - v_i}{h} \tag{2.1}$$

Equation 2.2 has a centered stencil and uses two points giving it a lower error, $\epsilon \approx h^2$.

$$dv_i = \frac{v_{i+1} - v_{i-1}}{2h} \tag{2.2}$$

Equation 2.3 uses a three point stencil, but due to the fact that the stencil is one sided it is still of the second order, $\epsilon \approx h^2$.

$$dv_i = \frac{4v_{i+1} - v_{i+2} + 3v_i}{2h} \tag{2.3}$$

Equation 2.4 uses a four point, centered stencil to produce a fourth order approximation, $\epsilon \approx h^4$. As seen in Figure 2.1 this is the most accurate as it has the lowest error and the steepest gradient such that a smaller smaller spacing gives a much higher reduction in error compared to that of the other stencils.

$$dv_i = \frac{-v_{i+2} + 8v_{i+1} - 8v_{i-1} + v_{i-2}}{12h} \tag{2.4}$$

2.2 Second Derivatives

Second derivatives are calculated in a similar manner to that of the first order and also have several variants depending on the stencil. It also uses the Taylor expansion to approximate the second derivative at a point such that $d^2v_i \approx \frac{df^2(x_i)}{dx^2}$.

The second ordered, centered stencil, seen in Equation 2.5, it is second order in h, which again means the error is relative to the spacing or $\epsilon \approx h^2$.

$$d^2v_i = \frac{v_{i+1} - 2v_i + v_{i-1}}{h^2} \tag{2.5}$$

The fourth ordered, centered stencil, seen in Equation 2.6 is more accurate than the second ordered, with $\epsilon \approx h^4$, but due to how complex it is compared to the second order, it is more expensive to calculate

$$d^2v_i = \frac{-v_{i+2} + 16v_{i+1} - 30v_i + 16v_{i-1} - v_{i-2}}{12h^2} \tag{2.6}$$

2.3 Ghost Points

The problem with FDMs, especially with those of a higher order, is their reliance on points on either side of the point being calculated. This is impossible closer to the function boundaries as the points needed to calculate the derivatives at these points are not within the bounds of the function. This can be overcome by the introduction of ghost points, points outside of the bounds of the function, but

which are still usable for the calculation of derivatives. These points are usually generated by treating the function as periodic over its domain and extending it as such, or by setting the points to zero. Both cases could lead to large errors in the approximation of the functions derivative if the points do not align with the actual points of the function at those positions.

Chapter 3

Time Integration

In this chapter, the evolution of an equation will be analyzed by looking at the time evolutions of two Partial Differential Equations (PDEs), namely the Advection Equation (Equation 3.1) and the Wave Equation (Equation 3.2).

$$\begin{aligned} u_t + cu_x &= 0, \qquad c \in \mathbb{R} \\ u(x,0) &= u_0(x) \end{aligned} \tag{3.1}$$

$$\begin{aligned} u_{tt} - c^2 u_{xx} &= 0, \qquad c \in \mathbb{R} \\ u(x,0) = u_0(x), &\qquad u_t(x,0) = p_0(x) \end{aligned} \tag{3.2}$$

3.1 Characteristic Structure

Characteristics are a way of simplifying an equation by changing the coordinates in which the PDE is calculated. It also shows how the information of the PDE propagates with time.

3.1.1 Advection Equation

The Advection Equation is a first order PDE (meaning the highest order derivative is in the first order). This means we need only specify one characteristic, p. Where $x = x(p)$ and $t = t(p)$ therefore $u = u(x,t) = u(x(p), t(p)) = u(p)$.

By the method of characteristics we can determine that the characteristic equations for the Advection equation are

$$\frac{dx}{dp} = c, \qquad \frac{dt}{dp} = 1, \qquad \frac{du}{dp} = 0 \tag{3.3}$$

which are then integrated to give

$$x = cp + C_1, \qquad t = p + C_2, \qquad u = C_3 \tag{3.4}$$

By setting $p = 0$ at $t = 0$, C_2 is set to 0 and $t = p$ everywhere. Setting $x = p$ along $u_0(x)$ gives us

$$x = cp + q \qquad \text{and} \qquad u = u_0(q). \tag{3.5}$$

$x = cp + q$ and $t = p$ can be used to give us the characteristic coordinate

$$q = x - ct \tag{3.6}$$

which is a line with a slope of c in the $(x, t) - plane$. Substituting this into u_0 gives us

$$u = u_0(x - ct) \tag{3.7}$$

3.1.2 Wave Equation

The Wave Equation is a second order PDE, therefore it has two characteristics. p and q.By reducing the equation to its canonical form, $u_{pq} = 0$. In this we see that

$$p = x - ct \qquad \text{and} \qquad q = x + ct \tag{3.8}$$

Since $u_{pq} = u_{qp} = 0$ then it follows that $u_p = P(p)$. Let $F(p)$ be an anti-derivative of P therefore $\frac{dF}{dp}(p) = P(p)$ and therefore

$$\frac{\partial}{\partial p}(u - F(p)) = 0 \tag{3.9}$$

by integrating both sides, it then follows that

$$u - F(p) = G(q) \tag{3.10}$$

and therefore by rearranging and substituting Equation 3.8, we get

$$u(x, t) = F(x - ct) + G(x + ct) \tag{3.11}$$

By analyzing this solution and comparing it to that of the Advection Equation, we see that we in fact get two characteristic coordinates which are lines with slopes of $\pm c$.

3.1.3 Spacing

Along with finding the characteristics comes the trouble of determining the spacing for the spacial and time axis when plotting. The spacial spacing will be denoted by h and time by k. If $h < k$ then the data needed to determine the value of the function at a given point in space and time will require data outside of the bounds of the stencil, conversely if $h > k$ then data between two spacial points is needed to calculate the next value, but this can be interpolated at the cost of calculation time and may yield a higher accuracy. The standard

is to set $h = k$ so that the stencil exactly fits the data needed to calculate the next point and every point being used need not be interpolated as it falls on an existing point in the spacing. This can be seen in the figures in Figure 3.1 for the Advection Equation and in Figure 3.2 for the Wave Equation.

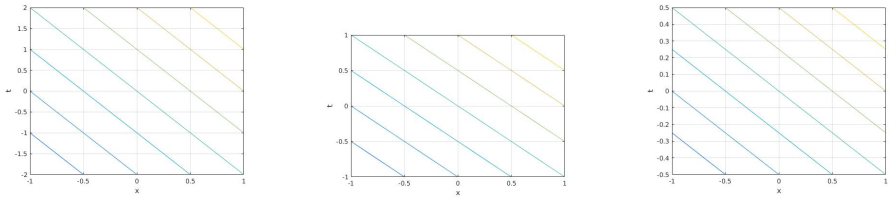

(a) $h < k$ (b) $h = k$ (c) $h > k$

Figure 3.1: Advection characteristic

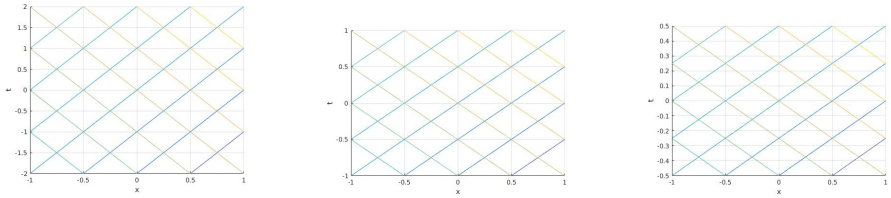

(a) $h < k$ (b) $h = k$ (c) $h > k$

Figure 3.2: Wave Equation Charactersitics

3.2 Discretization

Using the FDM discussed in Chapter 2 we will confirm the validity of three approximations of the advection equation, the Centered Euler, Leapfrog, and Upwind Euler methods, and the Leapfrog approximation of the wave equation.

3.2.1 Advection Equation

The advection equation can be approximated with the function v where

$$v_i^j = u(x_i, t_j) \tag{3.12}$$

by using the standard FDM we get the partial derivatives

$$\begin{aligned} \partial_x v_i^j &= \frac{v_{i+1}^j - v_{i-1}^j}{2h} + O(h^2) \\ \partial_t v_i^j &= \frac{v_i^{j+1} - v_i^{j-1}}{2k} + O(k^2) \end{aligned} \tag{3.13}$$

Leapfrog

Substituting Equation 3.13 into the advection equation we get

$$\partial_t v_i^j + c\partial_x v_i^j = 0 \tag{3.14}$$

however, v_i^{j+1} is unknown. So we rearrange the equation to solve for v_i^{j+1} to get

$$\begin{aligned} v_i^{j+1} &= v_i^{j-1} - 2ck\partial_x v_i^j \\ &= v_i^{j-1} - c\frac{k}{h}(v_{i+1}^j - v_{i-1}^j) + O(h^2k^2) \end{aligned} \tag{3.15}$$

This is known as the "Leapfrog" method as it requires v_i^{j-1} in order to calculate v_i^{j+1} This can be somewhat problematic with the initial data as $v_i^0 = u_0$ and v_i^2 onwards can be calculated this way but v_i^1 cannot be found by this method. Another problem concerining this method is the decoupling of odd and even points as all even points rely soley on the odd points of the previous time step and alternately for the odd points.

Centered Euler

The Centred Euler method seeks to circumvent this problem by setting

$$\partial_t v_i^j = \frac{v_i^{j+1} - v_i^j}{k} + O(k) \tag{3.16}$$

substituting this into the advection equation and rearranging to solve for v_i^{j+1} gives

$$\begin{aligned} v_i^{j+1} &= v_i^j - ck\partial_x v_i^j \\ &= v_i^j - c\frac{k}{2h}(v_{i+1}^j - v_{i-1}^j) + O(kh^2) \end{aligned} \tag{3.17}$$

This method uses a one-sided time step to calculate the next step. This makes it unconditionally unstable and over time it varies wildly from the actual data. Due to the error being relatively low for the first step, it is generally used to initialise the Leapfrog method.

Upwind Euler

By setting

$$\begin{aligned} \partial_x v_i^j &= \frac{v_{i+1}^j - v_i^j}{h} + O(h) \\ \partial_t v_i^j &= \frac{v_i^{j+1} - v_i^j}{k} + O(k) \end{aligned} \tag{3.18}$$

we get

$$\begin{aligned} v_i^{j+1} &= v_i^j - ck\partial_x v_i^j \\ &= v_i^j - c\frac{k}{h}(v_{i+1}^j - v_i^j) + O(kh) \end{aligned} \tag{3.19}$$

This is arguably the best method to calculate the advection equation as it uses a biased stencil to propel the data from u_0 along the t and x axis, much like the advection equation itself.

3.2.2 Wave Equation

Using the second order, second derivative FDM on u with $v_i^j = u(x_i, t_j)$ we get

$$\begin{aligned} \partial_{xx} v_i^j &= \frac{v_{i+1}^j - 2v_i^j + v_{i-1}^j}{h^2} + O(h^2) \\ \partial_{tt} v_i^j &= \frac{v_i^{j+1} - 2v_i^j + v_i^{j-1}}{k^2} + O(k^2) \end{aligned} \tag{3.20}$$

Substituting this into the wave equation we get

$$\partial_{tt} v_i^j - c^2 \partial_{xx} v_i^j = 0 \tag{3.21}$$

As with the advection equation, v_i^{j+1} is unknown. reaaringing to solve for this, we get

$$v_i^{j+1} = 2v_i^j - v_i^{j+1} + c^2 \frac{k^2}{h^2}(v_{i+1}^j - 2v_i^j + v_{i-1}^j) + O(h^2 k^2) \tag{3.22}$$

This is a Leapfrog method approximation similar to that of the advection equation, it however does not have the decoupling of points as this stencil uses three points from the previous time step as opposed to the two used by the advection equation. This method also has the problem of v_i^1 being needed as initial data, this can usually be solved by calculating the row by hand and then feeding it into the system as initial data.

3.3 Implimentation

The initial equation

$$u(x, 0) = e^{-x^2} \tag{3.23}$$

was calculated on the interval $-10 < x < 10$ and $0 < t < 20$ with 100 and 1000 data points and compared to the exact solution, the L2-norm of the error was also analysed. For each solution the ghost points were a periodic extension of the previous steps data. The results were as follows

3.3.1 Centered Euler Advection Equation

The exact solution to the equation is

$$u(x, t) = e^{-(x-t)^2} \tag{3.24}$$

The wild variance of the Centered Euler method can be seen after only two seconds in Figure 3.3. The L2-norm of the error exponentially increases over

time as seen in Figure 3.4. The method generates high frequency noise which is amplified over time and the previous step's noise feeds into the next step to be increased again. This is due to $k = h$ and how this step ratio sits exactly on the bounds what can be seen as a stable causal step. If $k < h$ the stability of the metod would increase greatly.

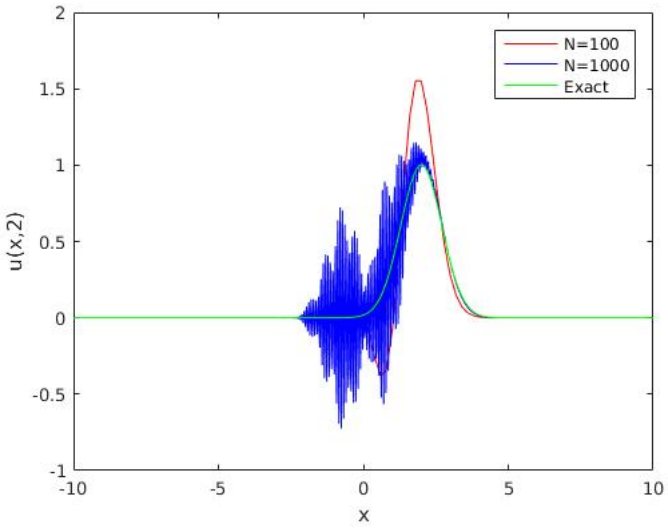

Figure 3.3: Advection Equation and Approximations after 2 seconds

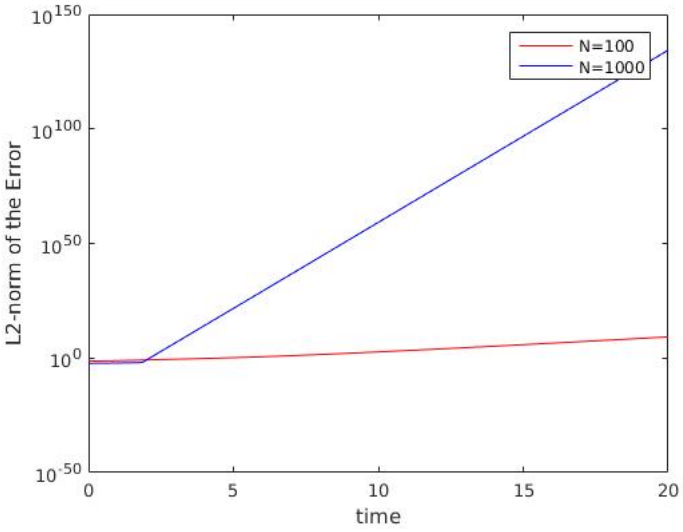

Figure 3.4: Change in L2-norm over time of Centered Euler Evolution

3.3.2 Leapfrog Advection Equation

The L2-norm of the error as seen in Figure 3.5 is due to the ghost points of the approximation being treated as a periodic extension of the function causing the function to be repeated every 20 time steps, the start of this can be seen in Figure 3.6, which shows the functions after nine time steps. The error seems, in the early steps, to be much smaller than expected, 10^{-15} instead of 10^{-4} and 10^{-8} for $N = 100$ and $N = 1000$ respectively. This is due to the ratio between the time, and spacial spacing being $k = h$, and that this perfectly projects the previous steps information to the next leading to a more precise approximation.

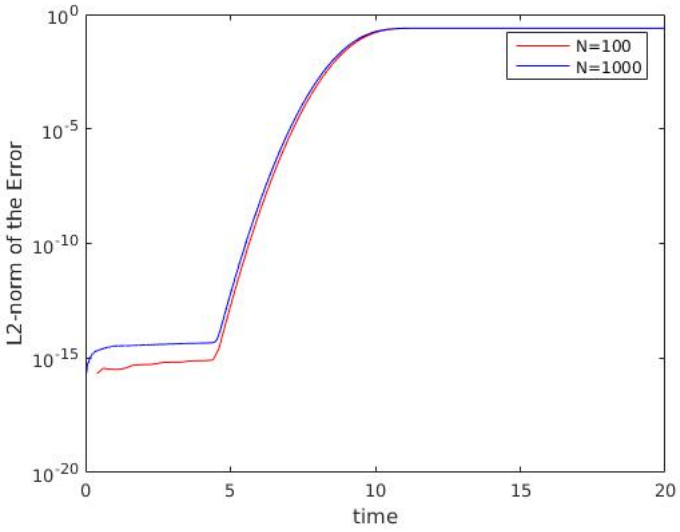

Figure 3.5: Change in L2-norm over time of Leapfrog Evolution

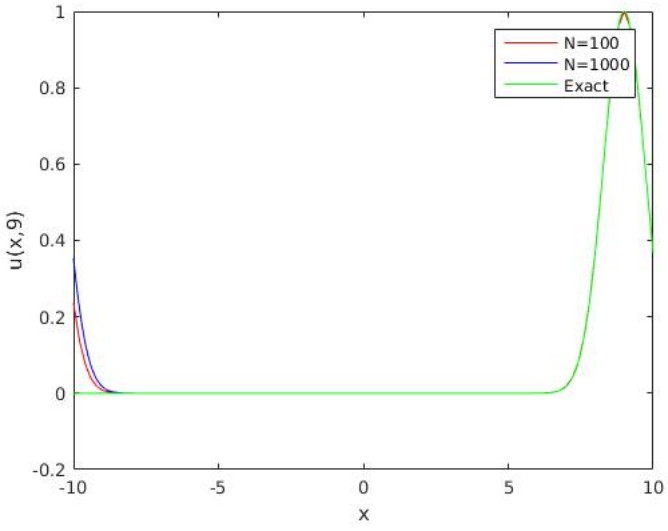

Figure 3.6: Advection Equation and Approximations after 9 seconds

3.3.3 Leapfrog Wave Equation

The d'Alembert solution to the equation is

$$u(x,t) = \frac{1}{2}(e^{-(x-t)^2} + e^{-(x+t)^2}) \tag{3.25}$$

Figure 3.10 shows how this approximation suffers from the same problem as the leapfrog advection approximation since it too has ghost points which see the function as a periodic extension and leads to the same problem of steps in the L2-norm of the error, shown in Figure 3.7. Adjusting the size of the time steps by making $k = 0.5h$ should leads to a minor reduction in the L2-norm of the error, however this is not the case as with $h = k$, the Leapfrog Wave Approximation has the same effect as that of the Leapfrog Advection Approximation where data is perefectly projected from one time step to the next leading it to be more accurate than that of a smaller time step as seen in Figure 3.8. With the large steps due to the periodic extension this is almost unnoticeable, if the time step is doubled to $k = 2h$ then the error increases exponentially over time after a relatively short period of time, seen in Figure 3.9.

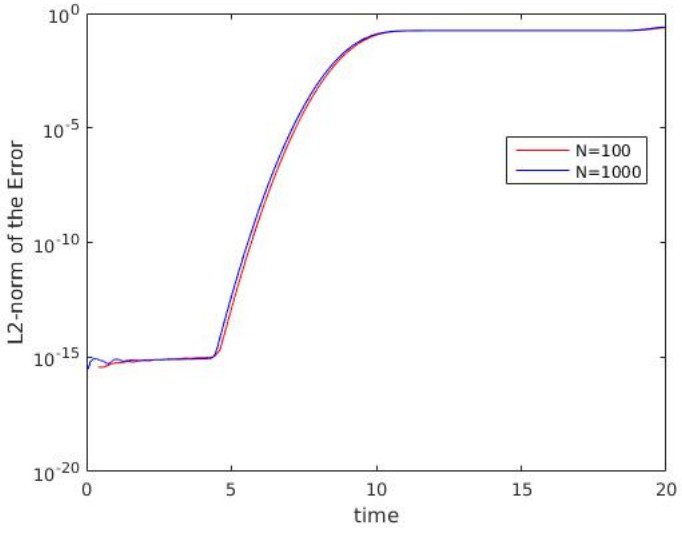

Figure 3.7: Change in L2-norm over time of Leapfrog Evolution with $k = h$

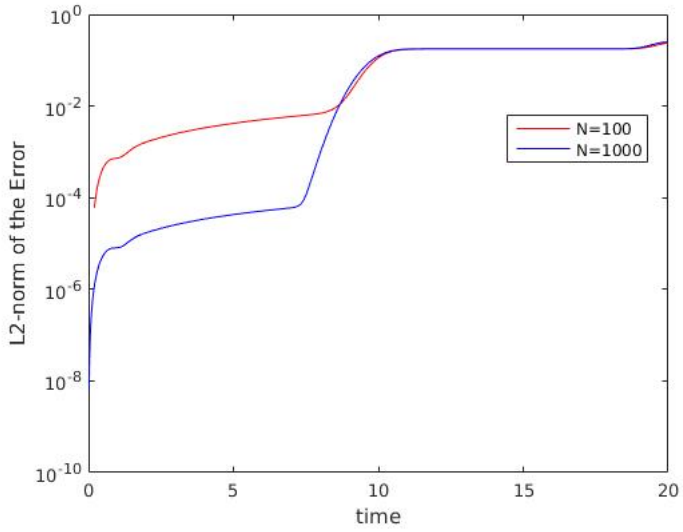

Figure 3.8: Change in L2-norm over time of Leapfrog Evolution with $k = 0.5h$

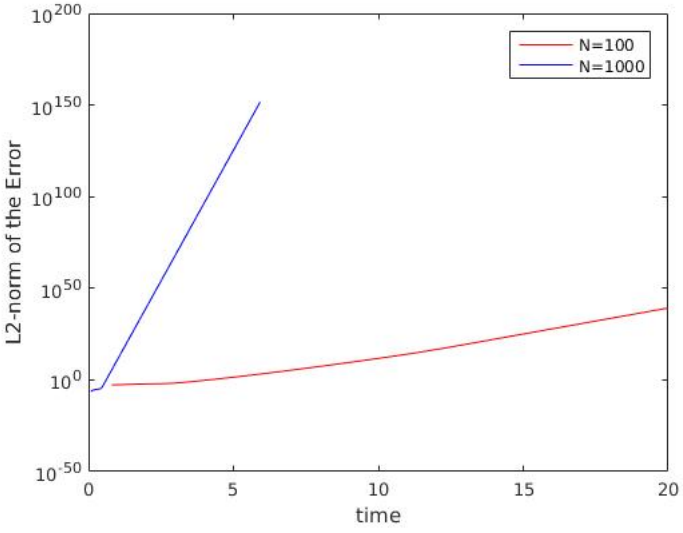

Figure 3.9: Change in L2-norm over time of Leapfrog Evolution with $k = 2h$

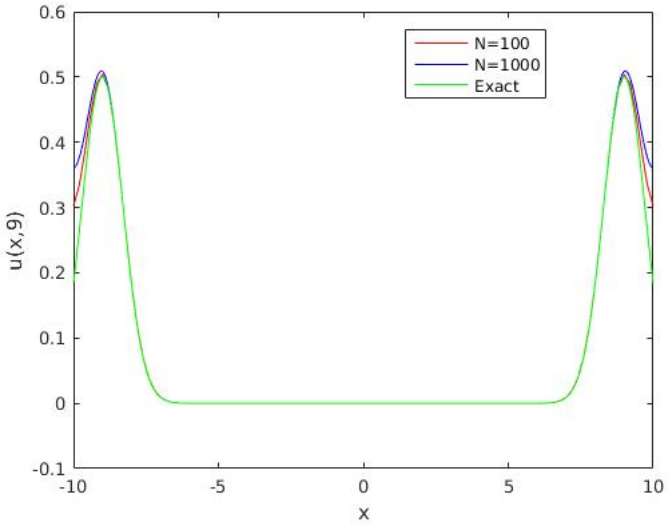

Figure 3.10: Wave Equation and Approximations after 9 seconds

By varying the spacial spacing size by setting $N = 2^i$ where $i = 6, \ldots, 12$ and fixing $k = 0.001$ we can deterimine the relationship between the spacing and the L2-norm of the error, looking at this relationship at $t = 5$ we get Figure 3.11. As seen here, the logarithmic scaling of both axis produces a line graph with a slope of -2. This is due to the fact that the error of the leapfrog is proportional to h^2, which, when logarithmicly scaled, goes as $2log(h)$, to produce the straight line.

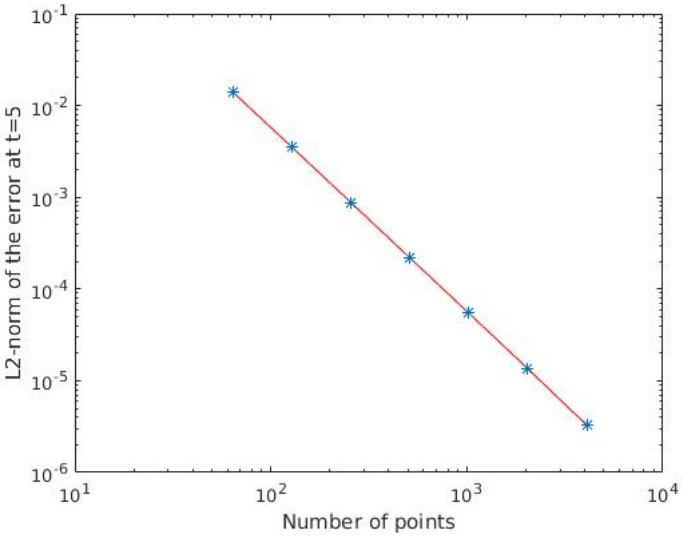

Figure 3.11: Change in the L2-norm of the error as the spacing varies

Chapter 4

Von Neumann Analysis

In this chapter we will discuss and analyze the stability of a discrete solution. We will do this by going over the Fourier transform and how it applies to the method. We will then discuss the amplification factor as well as its relation to dissipation and dispersion in a function. The analysis method will then be applied to the advection equation (4.1) and diffusion equation (4.2) and the results analyzed.

$$u_t + cu_x = 0, \qquad c \in \mathbb{R} \tag{4.1}$$

$$u_t - Ku_{xx} = 0, \qquad K \in \mathbb{R} \tag{4.2}$$

4.1 Fourier Transforms

Fourier transforms allow us to shift an equation from one which is in the spatial domain (x) to one which is in the frequency domain (ω). The general pair of equations for this is given as:

$$\begin{aligned} \mathcal{F}[f] = \hat{f}(\omega) &= \int_{-\infty}^{\infty} e^{-i\omega x} f(x) dx \\ \mathcal{F}^{-1}[\hat{f}] = f(x) &= \int_{-\infty}^{\infty} \frac{1}{2\pi} e^{i\omega x} \hat{f}(x) dx \end{aligned}$$

With the first equation being the Fourier transform of $f(x)$ to the frequency domain and the second being its inverse back to the spatial domain.

When applied to derivatives, Fourier transforms exhibit a useful property whereby the derivatives of the function in the spatial domain become complex polynomial scalings of the function in the frequency domain.

$$\begin{aligned} \mathcal{F}[\partial_x f] &= -i\omega x \hat{f} \\ \mathcal{F}[\partial_{xx}^2 f] &= -\omega^2 x \hat{f} \end{aligned}$$

This property gives us some insight into the nature of a function and its evolution. This can be seen by the analysis of the advection equation shown below. The magnitude of the Fourier transform of u, $\hat{u}$, is constant by the magnitude of the complex scalar C since $||e^{ic\omega t}|| = 1$, this indicates that it is stable as time evolves. s

$$\begin{aligned}
\mathcal{F}[u_t + cu_x] &= \mathcal{F}[0] \\
\hat{u}_t - i\omega c\hat{u} &= 0 \\
\frac{\hat{u}_t}{\hat{u}} &= i\omega c \\
\hat{u} &= Ce^{ic\omega t} \\
||\hat{u}|| &= ||Ce^{ic\omega t}|| \\
&= ||C|| \cdot ||e^{ic\omega t}|| \\
&= ||C||
\end{aligned}$$

Applying the same method to the diffusion equation shows that the function is dissipative over time due to its negative exponential relationship with ω. This means that the function loses energy over time.

$$\begin{aligned}
\mathcal{F}[u_t - ku_{xx}] &= \mathcal{F}[0] \\
\hat{u}_t + \omega^2 k\hat{u} &= 0 \\
\frac{\hat{u}_t}{\hat{u}} &= i\omega c \\
\hat{u} &= Ce^{-\omega^2 kt} \\
||\hat{u}|| &= ||Ce^{-\omega^2 kt}|| \\
&= ||C|| \cdot ||e^{-\omega^2 kt}|| \\
&= ||C||
\end{aligned}$$

4.2 The Amplification Factor

We can seek a similar analysis method as the one shown in Section 4.1 for difference methods. This is done by analyzing the stability of a difference scheme approximation with a single frequency. We start by assuming the following discrete solution form

$$v_j^n = \hat{v}^n(\omega)e^{i\omega x} = \hat{v}^n(\omega)e^{i\omega hj} \tag{4.3}$$

Now, using this into the difference scheme, we can attempt to (and will) find a recurrence relation for $\hat{v}^n$ such that

$$\hat{v}^{n+1} = \hat{Q}\hat{v}^n \tag{4.4}$$

This allows us to simplistically analyze the evolution of a function, as the nth step can be calculated as

$$\hat{v}^n = \hat{Q}\hat{v}^{n-1} = \hat{Q}^2\hat{v}^{n-2} = \cdots = \hat{Q}^n\hat{v}^0 \tag{4.5}$$

The value of $\hat{Q}$ for a specific frequency therefore determines how stable the difference scheme is.

$$\begin{aligned}
\hat{Q} > 1 &\Rightarrow ||\hat{v}^n|| = ||\hat{v}^0|| &\Rightarrow\text{Solution is unstable}\\
\hat{Q} < 1 &\Rightarrow ||\hat{v}^n|| < ||\hat{v}^0|| &\Rightarrow\text{Solution is stable, but dissipative}\\
\hat{Q} = 1 &\Rightarrow ||\hat{v}^n|| > ||\hat{v}^0|| &\Rightarrow\text{Solution is stable}
\end{aligned}$$

4.3 Examples

4.3.1 Centered Euler

$$v_j^{n+1} = v_j^n - c\frac{k}{2h}(v_{j+1}^n - v_{j-1}^n) + O(kh^2)$$

Substituting Equation 4.3

$$\begin{aligned}
\hat{v}^{n+1}e^{i\omega hj} &= \hat{v}^n e^{i\omega hj} - c\frac{k}{2h}(\hat{v}^n e^{i\omega h(j+1)} - \hat{v}^n e^{i\omega h(j-1)})\\
\hat{v}^{n+1}e^{i\omega hj} &= \hat{v}^n e^{i\omega hj} - c\frac{k}{2h}e^{i\omega hj}\hat{v}^n(e^{i\omega h} - e^{-i\omega h})\\
\hat{v}^{n+1} &= \hat{v}^n - ic\frac{k}{h}\hat{v}^n \sin\omega h\\
&= \hat{v}^n(1 - ic\frac{k}{h}\sin\omega h)
\end{aligned}$$

Now substituting Equation 4.4, we get

$$\begin{aligned}
\hat{Q}\hat{v}^n &= hatv^n(1 - ic\frac{k}{h}\sin\omega h)\\
\hat{Q} &= 1 - ic\frac{k}{h}\sin\omega h
\end{aligned}$$

Now, $||\hat{Q}|| = 1$ where $||1 - ic\frac{k}{h}\sin\omega h|| = 1$. Therefore $ic\frac{k}{h}\sin\omega h$ must be zero for it to be stable, meaning $\sin\omega h$ must be zero, which only occurs at $\omega = \frac{m\pi}{h}$ where $m \in \mathbb{Z}$. Since, in practice, the function is influenced by many small noisy frequencies, the solution will be unstable as $\hat{Q} > 1$ for these and their influence will compound over time due to this.

4.3.2 Upwind Euler

$$v_j^{n+1} = v_j^n - c\frac{k}{h}(v_{j+1}^n - v_j^n) + O(kh)$$

Substituting Equation 4.3

$$\hat{v}^{n+1}e^{i\omega hj} = \hat{v}^n e^{i\omega hj} - c\frac{k}{h}(\hat{v}^n e^{i\omega h(j+1)} - \hat{v}^n e^{i\omega hj})$$
$$\hat{v}^{n+1}e^{i\omega hj} = \hat{v}^n e^{i\omega hj} - c\frac{k}{h}\hat{v}^n e^{i\omega hj}(e^{i\omega h} - 1)$$
$$\hat{v}^{n+1}e^{i\omega hj} = \hat{v}^n e^{i\omega hj}(1 - c\frac{k}{h}(e^{i\omega h} - 1))$$
$$\hat{v}^{n+1} = \hat{v}^n(1 - c\frac{k}{h}(e^{i\omega h} - 1))$$

Now substituting Equation 4.4, we get

$$\hat{Q}\hat{v}^n = \hat{v}^n(1 - c\frac{k}{h}(e^{i\omega h} - 1))$$
$$\hat{Q} = 1 - c\frac{k}{h}(e^{i\omega h} - 1)$$

Let $c\frac{k}{h} = \alpha$

$$\begin{aligned}\hat{Q} &= 1 - \alpha(e^{i\omega h} - 1)\\ &= 1 - \alpha(\cos\omega h + i\sin\omega h - 1)\\ &= 1 - \alpha(\cos\omega h - 1) - \alpha i\sin\omega h\end{aligned}$$

Now, calculating the magnitude of $\hat{Q}$, gives us:

$$\begin{aligned}\hat{Q}^2 &= (1 - \alpha(\cos\omega h - 1) - \alpha i\sin\omega h)^2\\ &= (1 - \alpha(\cos\omega h - 1))^2 - (\alpha i\sin\omega h)^2\\ &= 1 - 2\alpha(\cos\omega h - 1) + \alpha^2(\cos\omega h - 1)^2 + \alpha^2\sin^2\omega h\\ &= 1 - 2\alpha(\cos\omega h - 1) + \alpha^2\cos^2\omega h - 2\alpha^2\cos\omega h + \alpha^2 + \alpha^2\sin^2\omega h\\ &= 1 - 2\alpha(\cos\omega h - 1) + 2\alpha^2 - 2\alpha^2\cos\omega h\\ &= 1 - 2\alpha(\cos\omega h - 1 + \alpha - \alpha\cos\omega h)\\ &= 1 - 2\alpha(1-\alpha)(\cos\omega h - 1)\end{aligned}$$

Therefore, for $||\hat{Q}|| \leq 1$, $1 - \alpha = 0$, and so:

$$\begin{aligned}1 - \alpha &\leq 0\\ 1 &\leq \alpha\\ 1 &\leq c\frac{k}{h}\\ \frac{h}{k} &\leq c\end{aligned}$$

Therefore the Upwind Euler method is stable when Courant's stability condition is met.

4.3.3 Leapfrog Advection Equation

$$v_j^{n+1} = v_j^{n-1} - c\frac{k}{h}(v_{j+1}^n - v_{j-1}^n)$$

Substituting Equation 4.3

$$\begin{aligned}
\hat{v}^{n+1}e^{i\omega hj} &= \hat{v}^{n-1}e^{i\omega hj} - c\frac{k}{h}(\hat{v}^n e^{i\omega h(j+1)} - \hat{v}^n e^{i\omega h(j-1)}) \\
&= \hat{v}^{n-1}e^{i\omega hj} - c\frac{k}{h}\hat{v}^n e^{i\omega hj}(e^{i\omega h} - e^{-i\omega h}) \\
\hat{v}^{n+1} &= \hat{v}^{n-1} - 2ic\frac{k}{h}\hat{v}^n \sin\omega h
\end{aligned}$$

Now substituting Equation 4.4 and remembering Equation 4.5 we get

$$\begin{aligned}
\hat{Q}^2\hat{v}^{n-1} &= \hat{v}^{n-1} - 2ic\frac{k}{h}\hat{Q}\hat{v}^{n-1}\sin\omega h \\
\hat{Q}^2 &= 1 - 2ic\frac{k}{h}\hat{Q}\sin\omega h \\
0 &= \hat{Q}^2 + 2ic\frac{k}{h}\sin(\omega h)\hat{Q} - 1 \\
\hat{Q} &= \frac{-2ic\frac{k}{h}\sin(\omega h) \pm \sqrt{(2ic\frac{k}{h}\sin(\omega h))^2 - 4(1)(-1)}}{2(1)} \\
&= -ic\frac{k}{h}\sin(\omega h) \pm \frac{\sqrt{4 - 4c^2\frac{k^2}{h^2}\sin^2(\omega h)}}{2} \\
&= -ic\frac{k}{h}\sin(\omega h) \pm \sqrt{1 - c^2\frac{k^2}{h^2}\sin^2(\omega h)}
\end{aligned}$$

Now, calculating the magnitude of $\hat{Q}$, gives us:

$$\begin{aligned}
\hat{Q}^2 &= \left(- ic\frac{k}{h}\sin(\omega h) \pm \sqrt{1 - c^2\frac{k^2}{h^2}\sin^2(\omega h)}\right)^2 \\
&= (-ic\frac{k}{h}\sin(\omega h))^2 + \left(\sqrt{1 - c^2\frac{k^2}{h^2}\sin^2(\omega h)}\right)^2 \\
&= c^2\frac{k^2}{h^2}\sin^2(\omega h) + 1 - c^2\frac{k^2}{h^2}\sin^2(\omega h) \\
&= 1
\end{aligned}$$

This shows that the Leapfrog is stable provided the square rooted term is real, this is only true if:

$$\begin{aligned} c^2\frac{k^2}{h^2}\sin^2(\omega h) &< 1 \\ c^2\frac{k^2}{h^2} &< 1 \\ c\frac{k}{h} &< 1 \\ c &< \frac{h}{k} \end{aligned}$$

Therefore the Leapfrog's stability also depends on Courant's stability condition is met.

4.3.4 Diffusion Equation

Using Equation 2.1 for the time derivative and Equation 2.5 for the second spatial derivative, we can transform the diffusion equation and solve for v_j^{n+1}. For the sake of removing confusion K will be replaced with C.

$$\begin{aligned} u_t - Cu_{xx} &= 0 \\ \frac{v_j^{n+1} - v_j^n}{k} - C\big(\frac{v_{j+1}^n - 2v_j^n + v_{j-1}^n}{h^2}\big) &= 0 \\ v_j^{n+1} - v_j^n &= kC\big(\frac{v_{j+1}^n - 2v_j^n + v_{j-1}^n}{h^2}\big) \\ v_j^{n+1} &= v_j^n + C\frac{k}{h^2}(v_{j+1}^n - 2v_j^n + v_{j-1}^n) \end{aligned}$$

Substituting Equation 4.3:

$$\begin{aligned} \hat{v}^{n+1}e^{i\omega hj} &= \hat{v}^n e^{i\omega hj} + C\frac{k}{h^2}(\hat{v}^n e^{i\omega h(j+1)} - 2\hat{v}^n e^{i\omega hj} + \hat{v}^n e^{i\omega h(j-1)}) \\ &= \hat{v}^n e^{i\omega hj} + C\frac{k}{h^2}\hat{v}^n e^{i\omega hj}(e^{i\omega h} - 2 + e^{-i\omega h}) \\ \hat{v}^{n+1} &= \hat{v}^n + C\frac{k}{h^2}\hat{v}^n(2\cos\omega h - 2) \\ &= (1 + 2C\frac{k}{h^2}(\cos\omega h - 1))\hat{v}^n \end{aligned}$$

Now substituting Equation 4.4 we get

$$\hat{Q} = 1 + 2C\frac{k}{h^2}(\cos\omega h - 1)$$

For $\hat{Q}$ to be stable and since $\cos\omega h - 1$ varies between 0 and -2

$$\begin{aligned} 2C\frac{k}{h^2} &< 1 \\ \frac{k}{h^2} &< \frac{1}{2C} \end{aligned}$$

This shows that in order for the method to be stable for each doubling of the number of spatial points, the number of time points must be quadrupled.